Experimental Evaluation of Coupling Coils for Underwater Wireless Power Transfer

Cândido Duarte
INESC TEC and FEUP
Porto, Portugal
candidoduarte@fe.up.pt

Francisco Gonçalves
INESC TEC and FEUP
Porto, Portugal
ee10196@fe.up.pt

Miguel Silva
INESC TEC and FEUP
Porto, Portugal
up201403909@fe.up.pt

Vasco Correia
INESC TEC and FEUP
Porto, Portugal
up201005211@fe.up.pt

Luís M. Pessoa
INESC TEC
Porto, Portugal
lpessoa@inesctec.pt

***Abstract*—In this work we focus on the influence of salt water as the medium between two coupling coils to design a wireless power transfer system. An electrical circuit model and an adequate characterization approach is presented to account for the power losses in the conductive medium. Optimum values for the load and efficiency of the power link are determined. Experimental results are provided to compare the performance of the coupling coils between different coupling mediums (air, fresh and salt water).**

***Index Terms*—seawater inductive link, underwater WPT**

I. Introduction

Deep-sea exploration faces so many adversities that may explain why it is often said that more than 95% of the ocean depth still remains unmapped and unexplored. For decades, oil and gas industries were the drivers of most explorations, but due to the great economic value of rare metals found in deep sea (e.g. in manganese nodules), commercial interest is emerging from mining industry as well [1]. Nevertheless, there are still several environmental concerns about this kind of activity [2], as there remains a great lack of information on the potential impact of the exploration in such a peculiar and rich biosphere.

Improving scientific knowledge on such a large underwater area requires a lot of inspection, sensing and tracking of different deap sea parameters, with the additional challenge of extremely harsh operating conditions. For convenience, to avoid human diving in the water, these monitoring tasks often imply the use of unoccupied submersible vehicles. Therefore, autonomous underwater vehicles (AUVs) are employed in missions that may last days or months, with virtually no remote assistance. These vehicles can be used to energize sensors located at deep seabed, conveniently without any wires involved in the process.

Fig. 1a illustrates this wireless power transfer (WPT) scenario in which the battery-operated AUV comprises a power inverter responsible for driving a coil under a specific resonance operation [3]–[5]. The inductive coupling is performed with a second coil, at the sensor, which rectifies the delivered power. Hence, as the AUV approaches the sensor platform, and as soon as a safe hoovering distance is reached, such WPT process is started. Fig. 1b depicts a representation of the resonant system (series resonance at the primary and secondary sides, through C_1 and C_2, respectively) together with a sketch of the concave geometry of the coils.

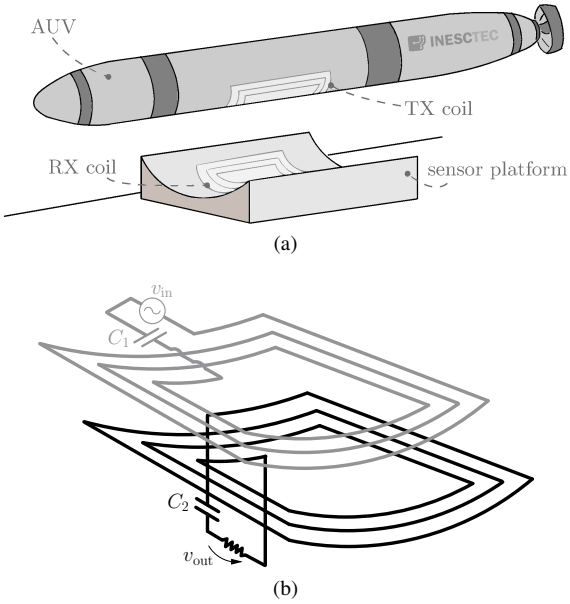

Fig. 1. Underwater WPT scenario. (a) AUV energizing sensor at seabed. (b) Sketch of the coupling coil system (AC equivalent).

The underwater magnetic resonant coupling using AUVs requires adequate form factors for the coil structures. Underwater WPT is usually conceived using cone docking, which implies that the solenoid is used as the preferred geometry [6]. For powering sensors underwater, by hovering the AUV close to the sensor, the geometry must be slightly different. In fact, in this type of application, the design of the coupling coils is very critical due to various reasons. First, the salt medium behaves as a conductor, dissipating power, hence the coil structure must take into account such losses. Also distance, orientation, and misalignments are all important variables that are difficult to accurately predict and keep static during the WPT process. The present work addresses the coupling coils taking into account such obstacles that degrade the WPT link efficiency.

This work is financed by the ERDF – European Regional Development Fund through the Operational Programme for Competitiveness and Internationalisation – COMPETE 2020 Programme and by National Funds through the Portuguese funding agency, FCT – Fundação para a Ciência e a Tecnologia within project POCI-01-0145-FEDER-031971.

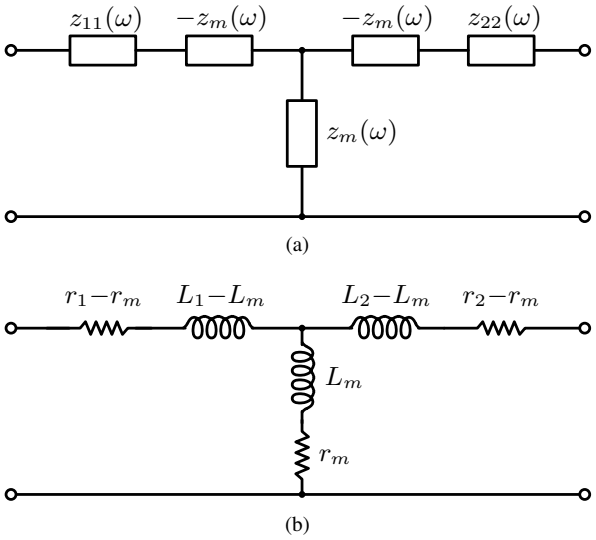

Fig. 2. Equivalent port network of the coupling coils with (a) z parameters and (b) with lumped elements.

II. Characterization of Coupling Coils

The coupling coils can be seen as a transformer and in general terms as a linear time invariant system characterized as a two-port electrical network. We adopt a Z-matrix approach to obtain the frequency-dependent impedance parameters of the coils, i.e. $z_{mn}(\omega)$ with $m, n = 1, 2$. Given the interchangeability of input and output without changing the response to an input stimulus, we admit the reciprocity theorem valid for coupling inductors [7]. Thus, we admit $z_{12}(\omega) = z_{21}(\omega)$, hereafter denoted as $z_m(\omega)$, and define the following symmetrical matrix

$$\mathbf{Z} = \begin{bmatrix} z_{11}(\omega) & z_m(\omega) \\ z_m(\omega) & z_{22}(\omega) \end{bmatrix} \tag{1}$$

in which

$$z_{11}(\omega) = r_1(\omega) + j\omega L_1(\omega) \tag{2}$$

$$z_{22}(\omega) = r_2(\omega) + j\omega L_2(\omega) \tag{3}$$

$$z_m(\omega) = r_m(\omega) + j\omega L_m(\omega) \tag{4}$$

The terms $L_1(\omega)$ and $L_2(\omega)$ represent the self inductance of primary and secondary sides, respectively, and $r_1(\omega)$ and $r_2(\omega)$ the associated parasitic resistances. Fig. 2a represents the circuit model as tee-equivalent representation of a generic reciprocal two-port network and Fig. 2b illustrates the respective lumped elements for the present case.

The quality factor for each n-side is given by

$$Q_n = \frac{\mathrm{Im}\{z_{nn}(\omega)\}}{\mathrm{Re}\{z_{nn}(\omega)\}} = \frac{\omega \cdot L_n}{r_n} \tag{5}$$

and the mutual inductive and resistive coupling factors [8] are respectively given as frequency-dependent quantities such as follows

$$k_i(\omega) = \sqrt{\frac{[\mathrm{Im}\{z_m(\omega)\}]^2}{\mathrm{Im}(z_{11}\{\omega)\}\mathrm{Im}\{z_{22}(\omega)\}}} = \frac{L_m(\omega)}{\sqrt{L_1(\omega) \cdot L_2(\omega)}} \tag{6}$$

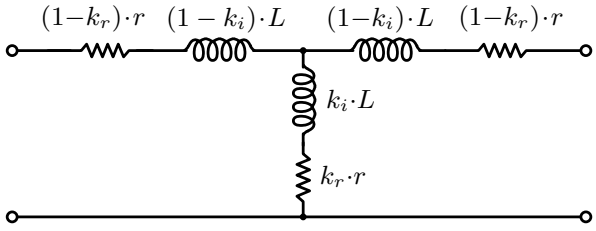

Fig. 3. Electrical model when the circuit is symmetrical, i.e. when $r_1(\omega)=r_2(\omega)=r(\omega)$ and $L_1(\omega)=L_2(\omega)=L(\omega)$.

$$k_r(\omega) = \sqrt{\frac{[\mathrm{Re}\{z_m(\omega)\}]^2}{\mathrm{Re}\{z_{11}(\omega)\} \cdot \mathrm{Re}\{z_{22}(\omega)\}}} = \frac{r_m(\omega)}{\sqrt{r_1(\omega) \cdot r_2(\omega)}} \tag{7}$$

If the coils are equal then the coupling system reduces to the one shown in Fig. 3. However, in our case, due to the different radius, the resultant coil properties differ, although slightly.

To characterize the coupling coils, an impedance meter is used first with each coil in open circuit, imposing $k_r(\omega) = k_i(\omega) = 0$, so that one can independently measure $z_1(\omega)$ and $z_2(\omega)$. Then, the input equivalent impedance $z_{\text{in}}(\omega)$ is measured from the primary side, with the secondary in short circuit, i.e. $z_{\text{in}}(\omega)|_{R_L=0}$, from which $z_m(\omega)$ is obtained

$$z_m(\omega) = \sqrt{\left[z_{11}(\omega) - z_{\text{in}}(\omega)\big|_{R_L=0}\right] \cdot z_{22}(\omega)} \tag{8}$$

The efficiency of the coupling coils, $\eta_{\text{link}}(\omega)$, with a series capacitance at resonance at each side, i.e. $\omega = \omega_0 = 1/(2\pi\sqrt{L_n C_n})$, is determined by

$$\eta_{\text{link}}(\omega_0) = \frac{P_{\text{out}}}{P_{\text{in}}} = \frac{R_L \cdot |I_{\text{out}}|^2}{R_{\text{in}}(\omega_0) \cdot |I_{\text{in}}|^2} = \frac{R_L}{R_{\text{in}}(\omega_0)} \cdot \left| \frac{z_m(\omega_0)}{r_2(\omega_0) + R_L} \right|^2 \tag{9}$$

where R_L represents the load at the secondary side and $R_{\text{in}}(\omega_0)$ is the resistance seen from the primary at resonance

$$R_{\text{in}}(\omega_0) = r_1(\omega_0) - \frac{r_m^2(\omega_0) - [\omega_0 L_m(\omega_0)]^2}{r_2(\omega_0) + R_L} \tag{10}$$

which leads to

$$\eta_{\text{link}} = \frac{R_L}{r_2(\omega_0) + R_L} \cdot \frac{r_m^2(\omega_0) + \omega_0^2 L_m^2(\omega_0)}{r_1(\omega_0) \cdot [r_2(\omega_0) + R_L(\omega_0)] - r_m^2(\omega_0) + \omega_0^2 L_m^2(\omega_0)} \tag{11}$$

The optimum load R_L^{opt} is obtained from (11) by imposing $\mathrm{d}\eta(\omega_0)/\mathrm{d}R_L = 0$, leading to

$$R_L^{\text{opt}}(\omega_0) = r_2(\omega_0) \cdot \sqrt{1 + k_i^2(\omega_0) Q_1 Q_2 - k_r^2(\omega_0)} \tag{12}$$

The optimum efficiency is obtained by replacing (12) in (11)

$$\eta_{\text{link}}^{\text{opt}}(\omega_0) = \frac{k_i^2(\omega_0) Q_1 Q_2 + k_r^2(\omega_0)}{\left(1 + \sqrt{1 + k_i^2(\omega_0) Q_1 Q_2 - k_r^2(\omega_0)}\right)^2} \tag{13}$$

which turns out to be slightly different from the case where r_m is neglected due to finite k_r [9].

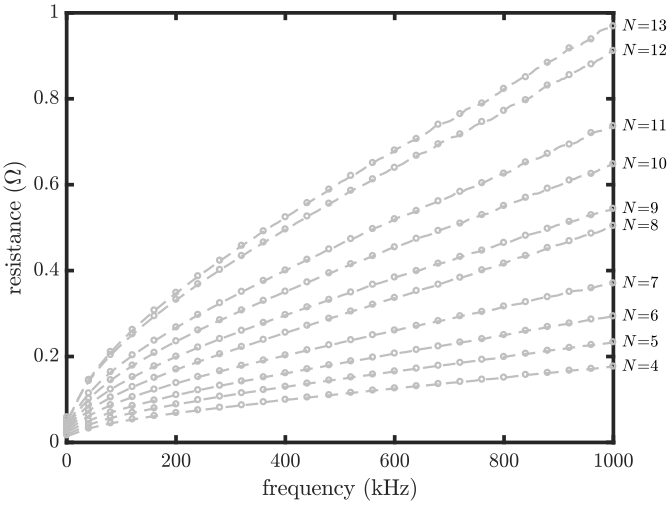

(a)

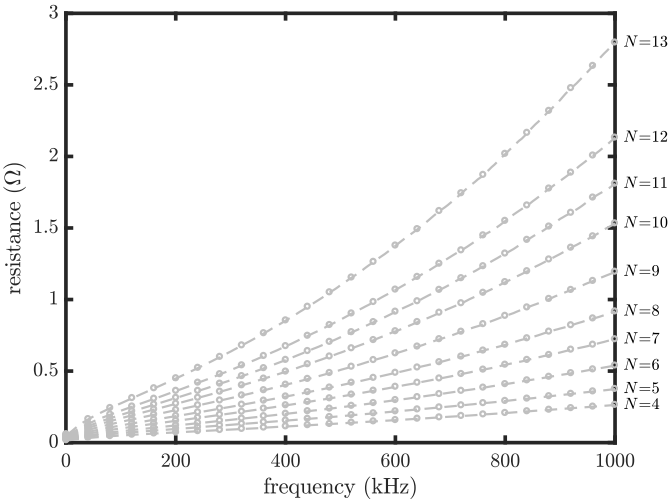

(b)

Fig. 4. Parasitic resistance measured for different number of turns of the coils with surrounding (a) air and (b) salt water.

III. Experimental Results

Our study makes use of coil housings for an AUV (20 cm diameter) where the minimum distance between the coils (properly encapsulated with epoxy) is about 4 cm. The magnet wire used in experiments consists of 14-AWG copper with 8.4 mΩ/m conduction resistance (at temperature 20°C). We have considered two concave structures with different number of turns (from 4 to 13) and measured their parasitic resistances along frequency up to 1 MHz using an impedance meter (Agilent E4980AL/102). Fig. 4(a) shows the results for air as the interface, and Fig. 4(b) shows the results when the salt water is included around the coils, taking into account a hollow cylinder filled with air, as shown in Fig. 5. It can be noticed that both in air and salt water, the coils have similar performance only up to about 100 kHz. Above such frequency value, in the presence of salt water a point of inflection is originated, which introduces a significant increase in slope.

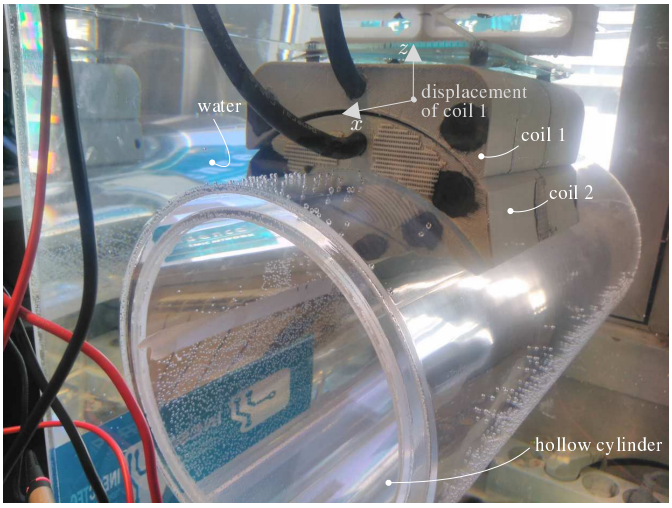

Fig. 5. Setup of coils for experiments. For the study of the coupling performance under different misalignments, coil 1 is placed at different distances x and z relative to coil 2.

This behavior has great implication on the unloaded quality factor (Q) for the coil when immersed in salt water, denoting an optimum value for Q.

In air, as the frequency increases, also the Q is increased because of the reduced rate of change in the parasitic resistance. However, with the salt water, the losses due to the conductivity of the medium counteract the Q improvement seen in air. We have measured two coils with 11 turns each (curvature length of 19 cm and width of 20 cm), in salt water and, to establish a straightforward comparison, we measured the same coils also in fresh water – coil 1 and coil 2 are very similar, except for a difference of 4 cm in the radius so that they can be employed in two different structures. Fig. 6(a) shows the quality factor measured for the coils – Q has been obtained from (5). As shown, in salt water, a peak value for Q occurs around the middle of the given frequency range, in contrast to the monotonically increasing Q of fresh water.

The coils in salt water have been displaced with different vertical (up to 3 cm) and lateral (10 cm) misalignments, with effect in the coupling factor. As a consequence, also the optimum frequency changes in terms of maximum link efficiency, as seen in Fig. 6(b). Moreover, in figure it is shown how the maximum efficiencies change along frequency in comparison with air and fresh water. Under perfect alignment of the coils, in salt water, the maximum efficiency is about 94% at 240 kHz. However, the peak value changes with the misalignment, and also the frequency at which such peak occurs. Nevertheless, this shows that high-frequency WPT can still be practical.

IV. Conclusion

The present work addressed the influence of the conductive medium in wireless power transfer for underwater applications. Optimum values were derived for the efficiency of the power link established by the inductive resonance of the coupling coils. It has been shown that the individual

TABLE I
DIFFERENCE LIST SUMMARY BETWEEN PERFORMANCES WITH AIR AND SALT BETWEEN THE COILS

	air	salt
quality factor	increases with frequency	has an optimum frequency for which Q is maximum
optimum load	$R_L^{\text{opt}} = r_2(\omega_0) \cdot \sqrt{1 + k_i^2(\omega_0) Q_1 Q_2}$	$R_L^{\text{opt}} = r_2(\omega_0) \cdot \sqrt{1 + k_i^2(\omega_0) Q_1 Q_2 - k_r^2(\omega_0)}$
maximum efficiency	$\eta_{\text{link}}^{\text{opt}}(\omega_0) = \frac{k_i^2(\omega_0) Q_1 Q_2}{\left(1+\sqrt{1+k_i^2(\omega_0) Q_1 Q_2}\right)^2}$	$\eta_{\text{link}}^{\text{opt}}(\omega_0) = \frac{k_i^2(\omega_0) Q_1 Q_2 + k_r^2(\omega_0)}{\left(1+\sqrt{1+k_i^2(\omega_0) Q_1 Q_2 - k_r^2(\omega_0)}\right)^2}$

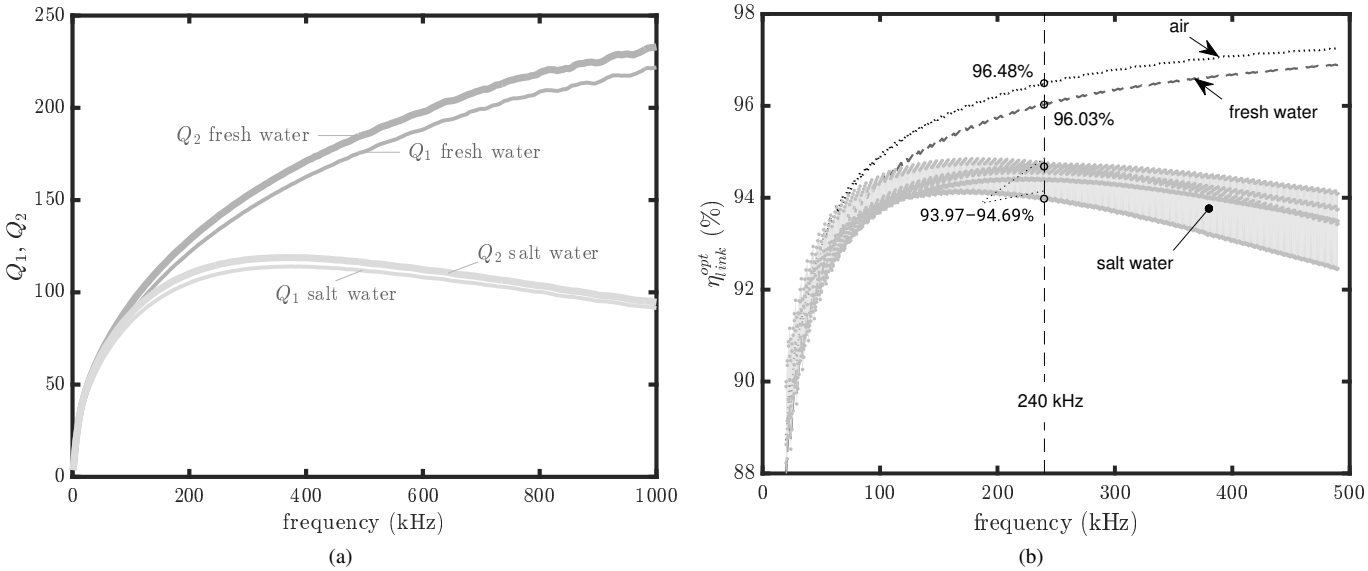

Fig. 6. Coil structure with 11 turns, in air and water. Data calculated from measurements: (a) quality factors Q_1 and Q_2, and (b) optimum efficiency on WPT between coils (shaded area is for salt water with and without misalignments).

quality factors are affected by the presence of salt in the water, starting to decrease with frequency at some point. This behavior is different from power transfer with air as the medium, where the quality factor increases always with frequency. Also, the optimum values for the load of the link and the respective maximum theoretical efficiency have been derived. Table I summarizes these results, in which the air interface is a particular case of null resistive coupling ($k_r = 0$). Performance evaluation has been presented also experimentally, with comparison of power transfer between different mediums, i.e. with air, fresh and salt water between the coils.

ACKNOWLEDGMENT

The authors would like to thank T. Ressurreição and R. Magno for all their help in lab setups. The authors acknowledge the assistance and resources made available by TEC4SEA in support of this work. This infrastructure is financed by FEDER funds through Programa Operacional Regional do Norte – NORTE 2020 and Programa Operacional Regional do Algarve – ALGARVE21, and by National funds through FCT – Fundação para a Ciência e a Tecnologia (NORTE-01-0145-FEDER-022097).

REFERENCES

[1] J. P. Clark and M. R. Neutra, "Mining manganese nodules: Potential economic and environmental effects," *Resources Policy*, vol. 9, no. 2, pp. 99–109, 1983.

[2] R. Sharma, "Environmental issues of deep-sea mining," *Procedia Earth and Planetary Science*, vol. 11, pp. 204–211, 2015.

[3] C. Duarte, F. Gonçalves, T. R. ao, R. Gomes, V. Correia, R. Gonçalves, and R. Santos, "A study on load modulation for underwater wireless power transfer," in *OCEANS*, Aberdeen, United Kingdom, Jun 2017, pp. 1–4.

[4] F. Gonçalves, C. Duarte, and L. M. Pessoa, "A novel circuit topology for underwater wireless power transfer," in *International Conference on Systems Informatics, Modelling and Simulation*, Riga, Latvia, Jun 2016, pp. 181–186.

[5] F. Gonçalves, A. Pereira, A. Morais, C. Duarte, R. Gomes, and L. M. Pessoa, "An adaptive system for underwater wireless power transfer," in *8th International Congress on Ultra Modern Telecommunications and Control Systems*, Lisbon, Portugal, Oct 2016, pp. 101–105.

[6] J.-G. Shi, D.-J. Li, and C.-J. Yang, "Design and analysis of an underwater inductive coupling power transfer system for autonomous underwater vehicle docking applications," *Journal of Zhejiang University SCIENCE C*, vol. 15, no. 1, pp. 51–62, Jan 2014.

[7] C. A. Desoer and E. S. Kuh, *Basic Circuit Theory*. McGraw-Hill, 1969.

[8] K. T. Ng, B. Rejaei, and J. N. Burghartz, "Substrate effects in monolithic RF transformers on silicon," *IEEE Transactions on Microwave Theory and Techniques*, vol. 50, no. 1, pp. 377–383, Jan 2002.

[9] T. Ressurreição, F. Gonçalves, C. Duarte, R. Gonçalves, R. Gomes, R. Santos, R. Esteves, P. Pinto, I. Oliveira, and L. M. Pessoa, "System design for wireless powering of AUVs," in *OCEANS*, Aberdeen, United Kingdom, Jun 2017, pp. 1–6.